Improving the width of lossy mode resonances (LMRs) in double-clad fibers

J.J. Imas, I. Del Villar, P. Zubiate, C. R. Zamarreño, I. R. Matías

***Abstract*— In this work, the characteristics of lossy mode resonances (LMRs) in double-clad fibers where the refractive index (RI) of the second cladding is lower than that of the first cladding are analyzed both numerically and experimentally. In the first place, the LMRs spectra obtained with a 75 nm TiO_2 thin film are simulated, and it is observed that a thicker second cladding improves the width of the resonances, making them narrower. Then, two experimental cases (no second cladding, and second cladding with thickness of 1.13 µm) are assessed, showing a good agreement with the previous simulations. Finally, an experimental refractometric study is carried out in liquids (surrounding medium refractive index in the 1.34 - 1.40 range) for both fibers, calculating the full width at 1dB (FW_{1dB}), the sensitivity, and the figure of merit (FOM). The FW_{1dB} is better for the LMR obtained on the fiber with second cladding while the sensitivity is slightly greater for the fiber without second cladding. In the case of the FOM, it is higher for the double-clad fiber as the narrowing of the resonances outweighs the lower sensitivity. These results show that the performance of LMR-based optical fiber sensors can be improved by employing double-clad fibers.**

***Index Terms*—lossy mode resonances (LMRs), thin films, full width half maximum (FWHM), figure of merit (FOM)**

I. Introduction

One of the concerns in the optical sensing field is how to improve the resolution of the devices so lower limits of detection can be achieved, for instance, in biosensing or chemical applications [1]–[3]. In the case of wavelength based optical sensors, the resolution depends on the minimum wavelength shift that can be measured with accuracy (in nm, pm) and the sensitivity of the device (nm/RIU, pm/RIU considering for instance a case in which the refractive index is being measured). The resolution (in RIU^{-1} for this example) is the ratio between these two parameters [4], [5].

When talking about the minimum wavelength shift that can be measured, it depends on the detector in the setup but also on the sensing device, a fact that is usually underestimated. If the resonance whose wavelength is being tracked is not narrow enough, the uncertainty in the position of the minimum or maximum will increase, so the minimum wavelength shift that can be measured with accuracy will be larger, even if the resolution of the detector is high. The simplest way to improve this (focusing exclusively on the sensing device) is to reduce the full width half maximum (FWHM) of the resonance.

Regarding lossy mode resonances (LMRs) [6]–[9], efforts to improve the resolution have been usually aimed at increasing the sensitivity. In fact, the two main options for this purpose have been to work at longer wavelengths in the near infrared (and even in the mid-infrared [10]), or to increase the refractive index (RI) contrast between the optical fiber (made of silica) and the material of the thin film [6], [11]. With respect to the FWHM, in [12] it is shown in a D-shaped fiber in reflection configuration that the FWHM can be controlled through the length of the nanocoating. By reducing its length through a laser ablation process, the FWHM is improved.

On the other hand, another suggested way to improve the performance in wavelength-based sensors with thin films is to include an intermediate layer between the waveguide and the thin film, where the RI of this additional layer is lower than that of the waveguide. In [13], it is numerically studied, in a Kretschmann configuration, the addition of a lithium fluoride (LiF) intermediate layer between the optical prism and the TiO_2 thin film that generates the LMR. This LiF layer reduces the FWHM of the resonances, improving the performance of the sensor.

With respect to fibers, this low RI intermediate layer becomes a second cladding between the first cladding and the thin film. This structure has been studied in the case of LPGs in [14] where it has been demonstrated that a low RI second cladding increases the sensitivity to the thin film thickness and to the surrounding medium refractive index (SRI) during the mode transition compared to a standard fiber with only one cladding. Furthermore, this increase in sensitivity is larger when the second cladding is thicker, but if it becomes too thick (around 0.8 µm), fading phenomena begin to appear.

The purpose of this work is to study, both numerically and experimentally, if LMRs performance in optical fibers can be improved in terms of figure of merit by adding a second low RI cladding between the first cladding and the thin film.

II. Materials and Methods

A. Fibers preparation: etching and deposition process

The employed fibers are double-clad fibers SMM900 from Fibercore. The first cladding has a diameter of 102 µm and a numerical aperture of 0.18, while the second cladding values are 124.7 µm and 0.24, respectively. Other relevant parameters of these fibers are the cut-off wavelength, which is 895 nm, and the modal field diameter of the core mode: 7.8 µm. From the fiber dimensions, it can be deduced that the initial thickness of the second cladding is 11.35 µm.

This work was supported by the Spanish Ministry of Universities through FPU18/03087 grant (Formación de Profesorado Universitario) and the Spanish Ministry of Science and Innovation through PID2019-106231RB-I00 TEC Research fund.

J.J Imas, I. Del Villar, P. Zubiate, C. R. Zamarreño and I. R. Matías are with the Institute of Smart Cities and the Department of Electrical, Electronic and Communications Engineering, Public University of Navarre, 31006 Pamplona, Spain (e-mail: josejavier.imas@unavarra.es; ignacio.delvillar@unavarra.es; pablo.zubiate@unavarra.es; carlos.ruiz@unavarra.es, natxo@unavarra.es)

In order to obtain fibers with different thicknesses of the second cladding, an etching process is required. A common etching process is based on using, for instance, a hydrofluoric acid (HF) solution and assuming a constant etching rate, but sometimes this technique is not precise enough. Therefore, a new strategy is introduced based on inscribing a long period grating (LPG) in the core of these fibers. In order to avoid any confusion, it must be remarked that other techniques could have been used to etch the fibers instead, but this method was selected because it enables to control the etching process with increased accuracy, despite making the structure more complex. It must also be said that the LPG is only employed in the etching process, and it does not play a role in the width of the LMRs, which is linked with the thickness of the second cladding (see the section III. Results and Discussion).

The LPG attenuation bands shift during the etching process, and a correlation has been established between this shift and the second cladding thickness based on numerical simulations performed with the software FIMMWAVE® (Photon Design Inc.), see the blue line in Fig. 1 (results obtained for 90 points simulated in the -1 µm - 11 µm thickness interval). The negative values of the second cladding thickness in Fig. 1 correspond to the situation where the second cladding has been totally etched and the etching process has started to affect the first cladding. The two points that are marked in red correspond to the two cases that will be studied in more detail in the results section.

The correlation shown in Fig. 1 corresponds to the shift of the resonance initially located around 1490 nm. The LPG has a period of 176 µm and length of 12.5 mm, which are the values employed in the simulations whose results are plotted in Fig. 1. The peak-to-peak refractive index modulation was set to 0.001 as it provided the best fitting between the depth of the experimental and theoretical LPG bands.

Regarding the LPGs writing process, the fibers were initially loaded with hydrogen, and then the LPGs were photo-inscribed point by point with a doubled argon laser, generating a quasi-square-wave profile with a 50% duty cycle. Finally, the fibers were stored for ten days to enable the out-diffusion of the remaining hydrogen and hence the grating stabilization. Then, for each of these fibers, a segment with a length of 30 mm (including the section where the LPG had been inscribed) was introduced in a plastic cuvette [15]. The cuvette was filled with 25% (v/v) hydrofluoric acid (Panreac). During the etching process, the shift of the LPG resonance was monitored, which required a SLD light source (FJORDx3 model, Pyroistech) to excite the core section of the fiber, and an optical spectrum analyzer (MS9740A, Anritsu). The etching process was stopped when the wavelength displacement approximately corresponded to the desired second cladding thickness.

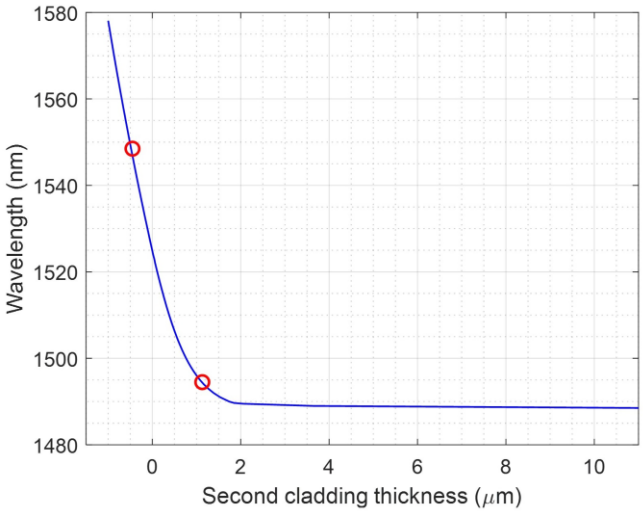

Fig. 1. Shift of the LPG attenuation band as a function of the second cladding thickness. The red points correspond to the experimental results.

Finally, a TiO_2 thin film was deposited on the fibers to generate the LMRs. An atomic layer deposition (ALD) system was employed, working at a constant temperature of 100 °C, and using ultrapure water and Tetrakis(dimethylamido)titanium(IV) (Sigma-Aldrich S.A) as precursors. A schematic diagram of the fiber and its different layers after this deposition is shown in Fig. 2. For the sake of clarity, the LPG inscribed in the fiber core is not included in Fig. 2, because it does not affect the width of the LMRs, the main focus of the current work.

B. Transmission measurements and refractometry

In order to measure the transmission spectra, the single mode fibers (SMF) under study are connected with a 200 µm temporary connector to a halogen light source (AQ4303B from ANDO) so light is transmitted both through the core and the cladding. A HR4000 spectrometer (Ocean Optics) for the 400 - 1000 nm range, and a NIRQuest spectrometer (Ocean Optics) for the 1000 - 1600 nm range, are used as detectors. It must be pointed out that LMRs are usually obtained through the deposition of a thin film of a material with suitable properties on a cladding removed multimode fiber [16]–[19] or on a D-shaped optical fiber [20]–[23], cases where the core is in contact or only separated by few micrometers from the thin film. Here, however, the core is isolated from the thin film by a cladding section of around 50 µm. Therefore, the LMR is generated through the interaction of the thin film with the light transmitted through the cladding, which is why it is required to use a halogen light source instead of a SLD light source, which would only excite the core section. On the other hand, as the core section is much smaller than that of the cladding, the light transmitted through the core does not have an impact on the transmission spectrum.

C. Simulations

For the simulations of the transmission spectra of the fibers, the plane wave method for a one-dimensional multilayer waveguide was applied [24]. This way, the transmission is calculated as the ratio between two integrals solved for the angles of incidence at the interface between the nanocoating and the substrate as shown in Eq. (1) [25], [26]. In this equation, $\theta_c(\lambda)$ is the critical angle, θ is the incidence

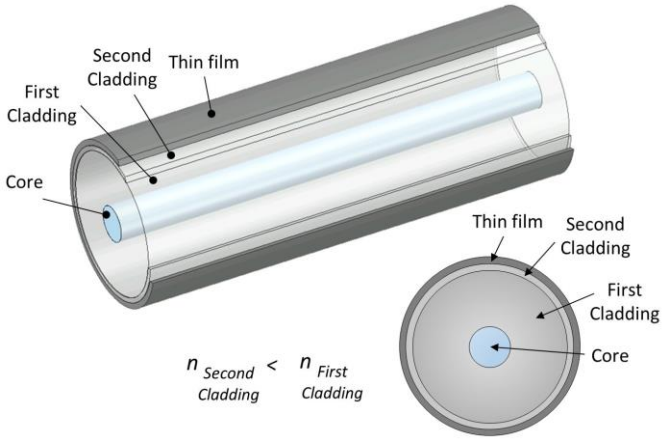

Fig. 2. Schematic diagram of a double-clad fiber with a thin film, including a close-up of its section.

angle, λ is the incidence wavelength, $N(\theta)$ is the number of reflections at the fiber TiO_2 interface, $p(\theta)$ is the power distribution of the optical source and $R(\theta,\lambda)$ is the reflection at the interface between the layer and the substrate for each θ and at each λ:

$$T(\lambda) = \frac{\int_{\theta_c(\lambda)}^{90º} p(\theta) R^{N(\theta)}(\theta,\lambda) d\theta}{\int_{\theta_c(\lambda)}^{90º} p(\theta)\, d\theta} \quad (1)$$

where $\theta_c(\lambda)$ is defined as:

$$\theta_c(\lambda) = \arcsin\left(\frac{n_{cl2}(\lambda)}{n_{cl1}(\lambda)}\right) \quad (2)$$

where n_{cl1} is the RI of the first cladding and n_{cl2} is the RI of the second cladding. The expression for $p(\theta)$ in Eq. (1) is given in Eq. (3) [25], [27], in which the broadband light source is modelled with a Gaussian distribution. In Eq. (3), W indicates the width of the Gaussian function, with W^2 equal to 0.005 rad as the value that best fits the numerical results with the experimental ones.

$$p(\theta) \alpha \exp\left[-\frac{\left(\theta - \frac{\pi}{2}\right)^2}{2W^2}\right] \quad (3)$$

Regarding the materials, the model for SiO_2 (optical fiber material) was obtained from [28] while the model for TiO_2 is based on ellipsometric measurements performed with an UVISEL 2 ellipsometer (Horiba Ltd.), see the real part of the TiO_2 refractive index (*n*) in Fig. 3. Regarding the imaginary part, *k*, of the thin film material, although the ellipsometric results provided a negligible value, it was necessary to consider for simulation purposes a non-zero value as, otherwise, no LMR was observed. The reason behind the obtained result is that the angle of incidence of the ellipsometer required to measure *n* with accuracy, around 70º, does not provide precise results for *k*. A value of 0.006 was chosen as it provides the best correlation between the experimental and the simulated results.

III. Results and Discussion

A. Comparison between simulations and experimental results

In the first place, the transmitted power corresponding to a double cladding fiber with a 75 nm TiO_2 thin film, is simulated as a function of the second cladding thickness (see the results in Fig. 4). The thickness of the second cladding is varied between 0 µm (no second cladding, standard fiber) and 1.2 µm in 0.2 µm steps.

Two LMRs can be observed in Fig. 4 for each of the studied cases. The LMR at shorter wavelengths (between 500 and 650 nm) corresponds to the transverse magnetic (TM) polarization and the one at larger wavelengths (between 1100 and 1400 nm) corresponds to the transverse electric (TE) polarization. It can be realized that the resonances become narrower, shift towards shorter wavelengths, and reduce their depth as the second cladding thickness increases. The most interesting result is that the width of the resonances improves with the thickness of the second cladding, so it is going to be studied if it is possible to experimentally reproduce it.

Two fibers with second cladding thicknesses of -0.45 µm and 1.13 µm, respectively, were obtained with the method described in section II.A. These thicknesses are the theoretical values given by the correlation in Fig. 1 considering the wavelength shift during the etching process. The two fibers are plotted as red open circles in Fig. 1. Then, a TiO_2 thin film with a thickness of 75 nm was deposited on the fibers.

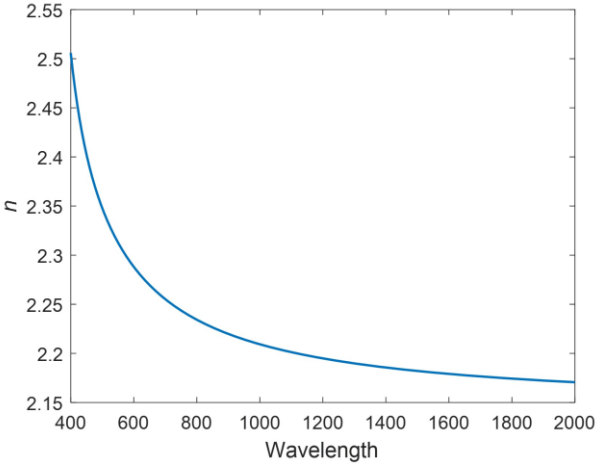

Fig. 3. Real part (*n*) of the TiO_2 refractive index measured with an ellipsometer.

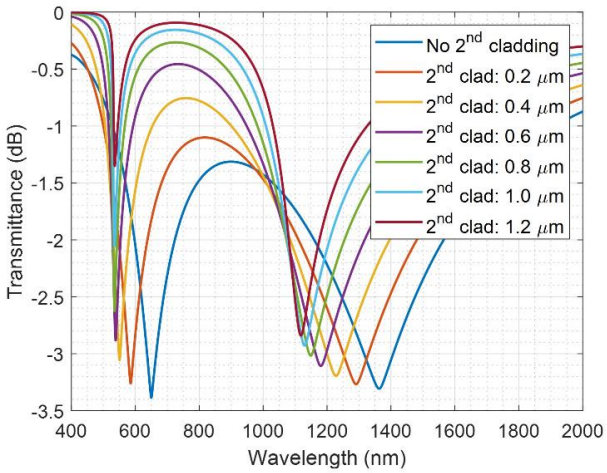

Fig. 4. Transmitted power obtained in simulations in a double-clad fiber with a 75 nm TiO_2 thin film as a function of the thickness of the second cladding.

The transmission spectra for both fibers are shown in Fig. 5, where the graph on the left shows the LMRs (TM polarization) in the 400 - 1000 nm range, while the graph on the right corresponds to the LMRs (TE polarization) in the 1000 - 1600 nm range. It is clear that the resonances are much narrower in the case of the fiber with a second cladding thickness of 1.13 µm than those corresponding to the fiber in which the second cladding has been completely etched. This happens for both the TM-polarized LMRs at shorter wavelengths and the TE-polarized LMRs at larger wavelengths. This result is confirmed by the FWHM values, which are included in Table 1. For the TM polarized LMR, the FWHM reduces by a factor of around 2 in the 1.13 µm case with respect to the 0 µm case (88 nm vs 161 nm). This factor increases up to almost 3.5 for the TE polarized LMR (172 nm vs 598 nm), but the resonances are much wider than for the TM polarization.

It is worth mentioning that, compared with previous literature [4], the obtained resonances in the case of the fiber with a second cladding are much wider than in the case of an LMR in a D-shaped fiber, but they still greatly improve the resonances that correspond to cladding removed multimode fibers.

The results in Fig. 5 qualitatively agree with the simulation shown in Fig. 4, that is, the FWHM becomes narrower when

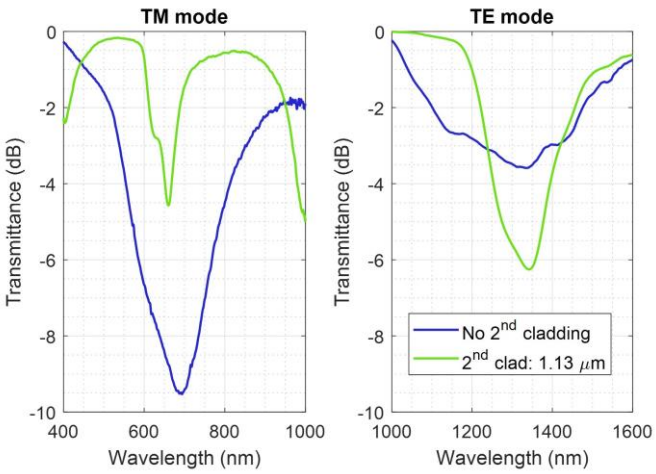

Fig. 5. Transmitted power in double-clad fibers with a TiO_2 thin film for two different thickness (-0.45 µm, and 1.13 µm).

Table 1. FWHM for the LMRs obtained in double-clad fibers.

Second cladding thickness (µm)	FWHM (nm)	
	TM polarized LMR	TE polarized LMR
0	161	598
1.13	88	172

increasing the thickness of the second cladding. Nevertheless, the results in Fig. 4 (numerical) and Fig. 5 (experimental) cannot be directly compared in terms of FWHM, as the resonances in Fig. 4 are not deep enough in some cases (less than 3 dB) to calculate the FWHM. The differences in the depth between the simulated and the experimental resonances are attributed to limitations in the simulation model. Even if values for $k > 0.01$ are employed (not realistic for TiO_2), which should increase the depth of resonances [11], they do not become much deeper. Modifying the light source parameters does not improve the depth of the resonances either.

In consequence, to perform a comparison between the experimental and numerical results, the full width at 1 dB (FW_{1dB} from here on) is calculated. The results are plotted in Fig. 6. Here, as opposed to Fig. 4, results for negative values of the second cladding (cases where the first cladding has also been slightly etched) are also included. However, it can be observed that the FW_{1dB} does not appreciably vary once the second cladding is totally etched. Although there are some differences, especially for the TE polarized LMRs, the experimental points are close to the respective tendency line, showing an agreement between experimental and simulated results.

It is also relevant to mention that the theoretical results for the TM polarized LMR show that there is a limit in the improvement that can be achieved in the width of the resonances. The minimum FW_{1dB} is attained for a second cladding thickness of 0.8 µm, and from that point, it starts to increase again.

B. Refractometric study

An experimental refractometric study in liquids was performed for the two experimental cases (with and without second cladding) varying the SRI from 1.341 to 1.398. The results are shown in Fig. 7, where Fig. 7a corresponds to the fiber without second cladding, and Fig. 7b to the fiber with a second cladding thickness of 1.13 µm. The same wavelength range (900 - 1700 nm) has been plotted for both Fig. 7a and Fig. 7b to enable a direct visual comparison between the width of

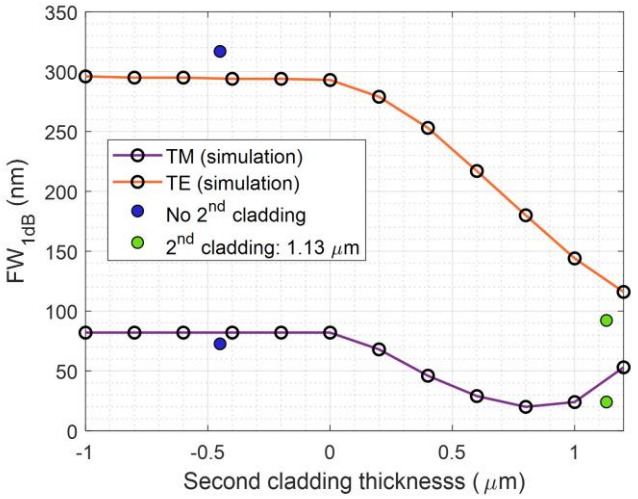

Fig. 6. FW_{1dB} as a function of the thickness for the simulated and the experimental results.

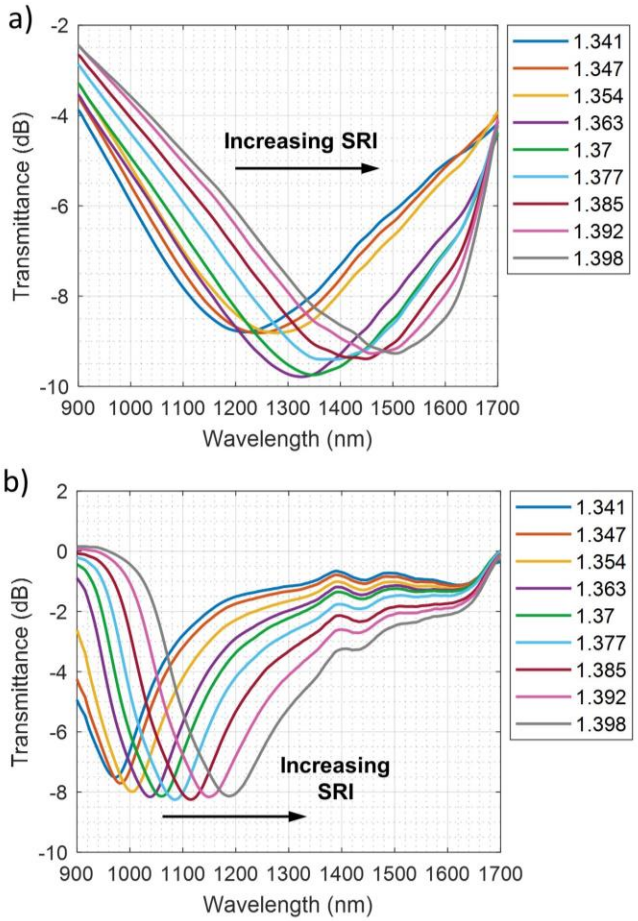

Fig. 7. Experimental refractometric study with the SRI varying in the 1.341 - 1.398 range. a) No second cladding, b) Second cladding 1.13 µm.

the resonances in both graphs. The LMRs that are plotted in Fig. 7 are the ones with TM polarization (initially located around 700 nm in air, see Fig. 5).

If the FW_{1dB} is plotted for both cases, see Fig. 8, the values are between two and four times lower in the case of the fiber with second cladding in all the studied SRI range, maintaining the better performance that has been previously observed in air. It has been decided to work with the FW_{1dB} instead of using the

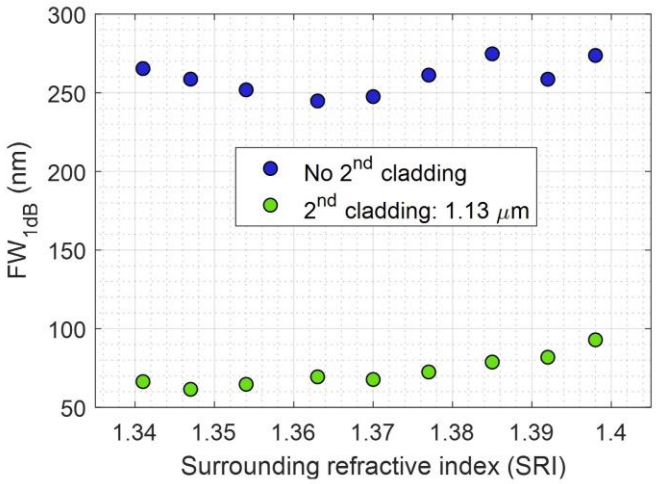

Fig. 8. FW_{1dB} (nm) of the LMR as a function of the SRI for the fiber without (blue points) and with second cladding (green points).

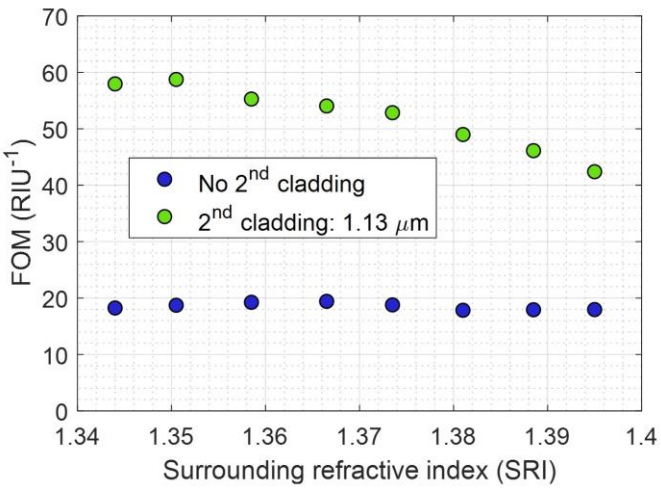

Fig. 10. FOM (RIU^{-1}) of the LMR as a function of the SRI for the fiber without (blue points) and with second cladding (green points).

standard FWHM because some LMRs do not present a parabolic shape, which negatively affects the calculus of the FWHM. For the fiber without second cladding, the FW_{1dB} oscillates between 250 and 300 nm. Regarding the fiber with second cladding, the FW_{1dB} increases from around 65 nm at 1.341 to around 100 nm at 1.398.

Regarding the sensitivity to the SRI, in Fig. 9, the LMR central wavelength vs the SRI is plotted for both fibers. It can be observed that in both cases the respective points can be approximated with accuracy ($R^2 = 0.998$ for the fiber without second cladding, and $R^2 = 0.985$ for the double-clad fiber) by a linear function. The slope of this function is the sensitivity (4782 nm/RIU, and 3707 nm/RIU, respectively), which can be considered constant in the whole studied SRI range. These results mean that the fiber without second cladding is superior to the double-clad fiber in terms of sensitivity to the SRI. In fact, it was expected that the difference in the sensitivities between both fibers would be higher based on the shift between air and SRI = 1.341 comparing Fig. 5 with Fig. 7. Both LMRs begin at around 700 nm in air, and the one corresponding to the fiber without second cladding shifts up to 1220 nm for SRI = 1.341, while the one with second cladding only shifts to 960 nm.

Finally, the figure of merit (FOM), defined in this case as the ratio between the sensitivity (constant value obtained from Fig. 9) and the FW_{1dB}, has been calculated for the two fibers, see Fig. 10. It can be seen that the FOM values are between two and three times higher for the fiber with a second cladding (values between 40 and 60 RIU^{-1}) than for the one without second cladding (values around 20 RIU^{-1}). This is due to the fact that the narrowing of the resonances in the fiber with second cladding outweighs the better performance in terms of sensitivity to the SRI of the fiber without second cladding. These results imply that the resolution of a device based on an LMR in a double-clad fiber will be better than that of a standard fiber without second cladding. It is also worth mentioning that the FOM decreases with the SRI in the double-clad fiber as the resonances become wider (see Fig. 7b and Fig. 8) while for the fiber without second cladding the FOM remains almost constant (the width of the resonances does not appreciably vary).

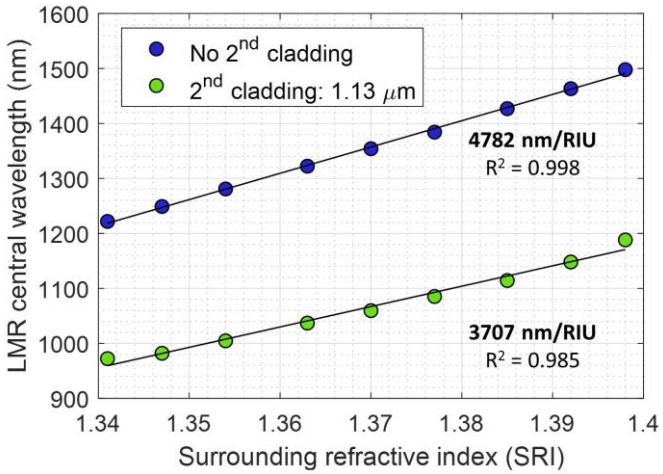

Fig. 9. LMR central wavelength as a function of the SRI for the fiber without (blue points) and with second cladding (green points). For each case, the points follow a linear trend whose slope is the sensitivity.

IV. Conclusion

In conclusion, the numerical and experimental results presented here point out to the fact that a better performance can be achieved in LMR-based optical fiber sensors by including an intermediate low RI second cladding between the first cladding and the thin film. This additional layer leads to narrower resonances, which mean obtaining sensors with a better resolution as the position of the resonance notch can be tracked with increased accuracy. However, the sensitivity slightly drops with a second cladding, although for the studied experimental cases the width of the resonances is what most impacts the FOM, having better results for a fiber with second cladding. Therefore, the results obtained here for LMRs in optical fibers point in the same direction as [13] (LMRs in a Kretschmann configuration) or [14] (LPGs, improving in this case the sensitivity instead of the FWHM), suggesting that intermediate low RI layers could be a game-changer in the development of optical sensors.

References

[1] X. D. Wang and O. S. Wolfbeis, "Fiber-optic chemical sensors and biosensors (2015-2019)," *Anal Chem*, vol. 92, no. 1, pp. 397–430, Jan. 2020, doi: 10.1021/acs.analchem.9b04708

[2] M. jie Yin, B. Gu, Q. F. An, C. Yang, Y. L. Guan, and K. T. Yong, "Recent development of fiber-optic chemical sensors and biosensors: Mechanisms, materials, micro/nano-fabrications and applications,"

Coord Chem Rev, vol. 376, pp. 348–392, Dec. 2018, doi: 10.1016/J.CCR.2018.08.001.

[3] A. B. Socorro-Leránoz, D. Santano, I. del Villar, and I. R. Matias, "Trends in the design of wavelength-based optical fibre biosensors (2008–2018)," *Biosensors and Bioelectronics: X*, vol. 1. Elsevier Ltd, Jun. 01, 2019. doi: 10.1016/j.biosx.2019.100015.

[4] A. Urrutia, I. del Villar, P. Zubiate, and C. R. Zamarreño, "A Comprehensive Review of Optical Fiber Refractometers: Toward a Standard Comparative Criterion," *Laser Photon Rev*, vol. 13, no. 11, p. 1900094, Nov. 2019, doi: 10.1002/lpor.201900094.

[5] F. Chiavaioli, C. A. J. Gouveia, P. A. S. Jorge, and F. Baldini, "Towards a Uniform Metrological Assessment of Grating-Based Optical Fiber Sensors: From Refractometers to Biosensors," *Biosensors 2017, Vol. 7, Page 23*, vol. 7, no. 2, p. 23, Jun. 2017, doi: 10.3390/BIOS7020023.

[6] I. del Villar *et al.*, "Optical sensors based on lossy-mode resonances," *Sens Actuators B Chem*, vol. 240, pp. 174–185, Mar. 2017, doi: 10.1016/J.SNB.2016.08.126.

[7] F. Chiavaioli and D. Janner, "Fiber Optic Sensing with Lossy Mode Resonances: Applications and Perspectives," *Journal of Lightwave Technology*, vol. 39, no. 12, pp. 3855–3870, Jun. 2021, doi: 10.1109/JLT.2021.3052137.

[8] Q. Wang and W. M. Zhao, "A comprehensive review of lossy mode resonance-based fiber optic sensors," Optics and Lasers in Engineering, vol. 100. Elsevier Ltd, pp. 47–60, Jan. 01, 2018. doi: 10.1016/j.optlaseng.2017.07.009.

[9] N. Paliwal and J. John, "Lossy Mode Resonance (LMR) Based Fiber Optic Sensors: A Review," IEEE Sens J, vol. 15, no. 10, pp. 5361–5371, Oct. 2015, doi: 10.1109/JSEN.2015.2448123.

[10] I. Vitoria et al., "Beyond near-infrared lossy mode resonances with fluoride glass optical fiber," Optics Letters, Vol. 46, Issue 12, pp. 2892-2895, vol. 46, no. 12, pp. 2892–2895, Jun. 2021, doi: 10.1364/OL.428533.

[11] I. del Villar et al., "Design rules for lossy mode resonance based sensors," Appl Opt, vol. 51, no. 19, pp. 4298–4307, Jul. 2012, doi: 10.1364/AO.51.004298.

[12] O. Fuentes et al., "Improving the width of lossy mode resonances in a reflection configuration D-shaped fiber by nanocoating laser ablation," Opt Lett, vol. 45, no. 17, p. 4738, Sep. 2020, doi: 10.1364/ol.402177.

[13] Y. Zhang et al., "Theoretical modeling and investigations of lossy mode resonance prism sensor based on TiO2 film," Optics Express, Vol. 30, Issue 18, pp. 32483-32500, vol. 30, no. 18, pp. 32483–32500, Aug. 2022, doi: 10.1364/OE.466170.

[14] I. del Villar et al., "Tunable sensitivity in long period fiber gratings during mode transition with low refractive index intermediate layer," Journal of Lightwave Technology, pp. 1–10, 2022, doi: 10.1109/JLT.2022.3226800.

[15] I. del Villar, O. Fuentes, F. Chiavaioli, J. M. Corres, and I. R. Matias, "Optimized strain long-period fiber grating (LPFG) sensors operating at the dispersion turning point," *Journal of Lightwave Technology*, vol. 36, no. 11, pp. 2240–2247, Jun. 2018, doi: 10.1109/JLT.2018.2790434.

[16] M. Hernáez, I. del Villar, C. R. Zamarreño, F. J. Arregui, and I. R. Matias, "Optical fiber refractometers based on lossy mode resonances supported by TiO2 coatings," *Appl Opt*, vol. 49, no. 20, pp. 3980–3985, Jul. 2010, doi: 10.1364/AO.49.003980.

[17] C. R. Zamarreño, Z. Zamarreño, M. Hernaez, I. del Villar, I. R. Matias, and F. J. Arregui, "Tunable humidity sensor based on ITO-coated optical fiber," *Sensors and Actuators B*, vol. 146, pp. 414–417, 2010, doi: 10.1016/j.snb.2010.02.029.

[18] P. Niedziałkowski *et al.*, "Electrochemical performance of indium-tin-oxide-coated lossy-mode resonance optical fiber sensor," *Sens Actuators B Chem*, vol. 301, p. 127043, Dec. 2019, doi: 10.1016/J.SNB.2019.127043.

[19] M. Hernaez, A. G. Mayes, and S. Melendi-Espina, "Lossy Mode Resonance Generation by Graphene Oxide Coatings Onto Cladding-Removed Multimode Optical Fiber," *IEEE Sens J*, vol. 19, no. 15, pp. 6187–6192, Aug. 2019, doi: 10.1109/JSEN.2019.2906010.

[20] P. Zubiate, C. R. Zamarreño, I. Del Villar, I. R. Matias, and F. J. Arregui, "High sensitive refractometers based on lossy mode resonances (LMRs) supported by ITO coated D-shaped optical fibers," *Opt Express*, vol. 23, no. 6, p. 8045, Mar. 2015, doi: 10.1364/oe.23.008045.

[21] F. J. Arregui, I. Del Villar, C. R. Zamarreño, P. Zubiate, and I. R. Matias, "Giant sensitivity of optical fiber sensors by means of lossy mode resonance," *Sens Actuators B Chem*, vol. 232, pp. 660–665, Sep. 2016, doi: 10.1016/j.snb.2016.04.015.

[22] C. L. Tien, H. Y. Lin, and S. H. Su, "High Sensitivity Refractive Index Sensor by D-Shaped Fibers and Titanium Dioxide Nanofilm," *Advances in Condensed Matter Physics*, vol. 2018, 2018, doi: 10.1155/2018/2303740.

[23] G. Moro *et al.*, "Nanocoated fiber label-free biosensing for perfluorooctanoic acid detection by lossy mode resonance," *Results in Optics*, vol. 5, p. 100123, Dec. 2021, doi: 10.1016/J.RIO.2021.100123.

[24] A. Yariv, P. Yeh, and C.-S. Hong, "Electromagnetic propagation in periodic stratified media. I. General theory*," *JOSA, Vol. 67, Issue 4, pp. 423-438*, vol. 67, no. 4, pp. 423–438, Apr. 1977, doi: 10.1364/JOSA.67.000423.

[25] I. del Villar *et al.*, "Generation of lossy mode resonances by deposition of high-refractive-index coatings on uncladded multimode optical fibers," *Journal of Optics*, vol. 12, no. 9, Sep. 2010, doi: 10.1088/2040-8978/12/9/095503.

[26] A. K. Sharma and B. D. Gupta, "On the sensitivity and signal to noise ratio of a step-index fiber optic surface plasmon resonance sensor with bimetallic layers," *Opt Commun*, vol. 245, no. 1–6, pp. 159–169, Jan. 2005, doi: 10.1016/J.OPTCOM.2004.10.013.

[27] I. del Villar, V. Torres, and M. Beruete, "Experimental demonstration of lossy mode and surface plasmon resonance generation with Kretschmann configuration," *Optics Letters, Vol. 40, Issue 20, pp. 4739-4742*, vol. 40, no. 20, pp. 4739–4742, Oct. 2015, doi: 10.1364/OL.40.004739.

[28] I. H. Malitson, "Interspecimen Comparison of the Refractive Index of Fused Silica," *J Opt Soc Am*, vol. 55, no. 10, p. 1205, Oct. 1965, doi: 10.1364/josa.55.001205.